Performance Evaluation of Millimeter Wave Full-Duplex Cellular Networks

Hernán-Felipe Arraño-Scharager[(1),(2)], Jean-Marc Kelif[(1)], and Marceau Coupechoux[(2)]
(1) Orange Labs Networks, 44 Avenue de la République, 92320 Châtillon, France
(2) LTCI, Telecom ParisTech, University Paris-Saclay, France

***Abstract*—The idea of implementing full-duplex (FD) under a millimeter wave (mmWave) context can be jointly beneficial, as FD may enhance the spectral efficiency of mmWave systems, and on the other hand, a beamforming-based mmWave model can help reduce the excessive co-channel interference experienced in traditional sub-6 GHz FD networks. In this paper, we investigate the possibility for base stations (BSs) to switch between half-duplex (HD) and FD, as it is proposed in sub-6 GHz to reduce interference, while users equipment and BSs employ beamforming techniques. The system is analyzed using stochastic geometry and realistic models are used to validate its performance. Results show that contrary to sub-6 GHz, an hybrid FD/HD network is not required in mmWave. We also show that reducing the transmission power of FD BSs avoids uplink spectral efficiency degradation, while still enabling a downlink enhancement with respect to a HD deployment.**

***Index Terms*—5G; Full-Duplex; Millimeter Wave; Stochastic Geometry**

I. Introduction

Using millimeter wave (mmWave) bands may help increase the available system's bandwidths and offload the currently saturated spectrum. Moreover, massive multiple-input multiple-output (MIMO), 3D beamforming and full-duplex (FD) are also considered as techniques that may meet next-generation expectations. In this regard, MIMO and 3D beamforming technologies can directly cope the degradation experienced in mmWaves propagation by steering the signals towards the intended receiver. Simultaneously, mmWave adoption can improve the feasibility of massive MIMO systems, as smaller wavelengths enable the utilization of smaller antennas, allowing to place bigger antenna arrays in smaller surfaces.

FD transceivers can simultaneously receive and transmit on the same frequency band, theoretically doubling the average spectral efficiency (ASE). However, if applied in a current sub-6 GHz cellular context, FD transmissions end up being interfered by excessive co-channel interference coming from either base stations (BSs) or users equipment (UEs) employing the same radio resource. As a consequence, even if the overall network performance may be improved, uplinks (ULs) are usually degraded [1], preventing so far the deployment of FD. Thus, the idea of implementing FD under a mmWave context can be jointly beneficial, as FD may enhance the spectral efficiency (SE) of mmWave systems, and on the other hand, a beamforming-based mmWave model can help reduce the interference of FD in sub-6 GHz networks.

In this paper we propose and analyze a novel beamforming-based mmWave cellular system where BSs can adopt FD or HD modes. We study the optimal proportion of FD and HD BSs and we investigate a power control scheme for FD BSs.

A. Related Works

The performance of "hybrid" cellular networks in which BSs are half-duplex (HD) and FD capable, as a means to cope the excessive interference in sub-6 GHz, has been studied by several scholars [1]–[4]. Authors in [1] propose a duplex-switching policy for BSs based on the position of the scheduled users. This policy enables to reduce the UL degradation, without affecting too much the downlink (DL) performance. In [4], users decide the duplex-mode based on the received power from their serving BSs. Results show that the network sum data rate can be improved with respect to both FD- and HD-systems by adopting an hybrid scheme. Motivated by this works, we investigate the need of hybrid-duplex techniques in mmWave environments.

Regarding the use of stochastic geometry to analyze HD-based mmWave cellular systems, authors in [5] use a distance-dependent line-of-sight (LOS) probability function and propose to model the locations of the LOS and non-LOS (NLOS) BSs as Poisson point processes (PPPs). Similarly, in [6] a LOS ball approximation is used, yet larger transmission bandwidths and Log-Normal shadowing are considered. Actual building locations are used to validate the results. In [7], a blockage model is also considered. Closed-form expressions are obtained thanks to a two ball approximation. Further, in [8] an overview of mathematical models is provided. Results show that mmWave systems are in general significantly more noise-limited than sub-6 GHz ones, self-backhauling is more viable and that operators can benefit from sharing their spectrum.

The potential and applicability of FD mmWave-based cellular networks has been addressed in recent works [9]–[13]. Particularly, in [9], results show that an antenna with separate arrays for transmission and reception favors the self-interference cancellation (self-IC) versus cost and surface, if compared to a single array model. In [13], several suboptimal solutions are proposed to the joint transmission and reception beamforming problem, to maximize the achievable rate. Results show the feasibility of FD mmWave communications due to the robustness against the geometry of antenna arrays and channel estimation errors. However, to the best of our knowledge, an hybrid-duplex stochastic geometry-based analysis has not yet been proposed nor analyzed.

B. Contributions

Our contributions in this paper are the following:

- We model a mmWave hybrid-duplex cellular network using the theory of stochastic geometry, deriving analytical expressions for the coverage probability and ASE.
- We model the residual self-interference (RSI) in FD-enabled elements by considering the geometry of the transmitted and received beams in the BSs.
- We investigate the need to implement an hybrid FD/HD scheme in mmWave environments and show that contrary to sub-6 GHz, hybrid schemes are not required.
- We investigate the advantage of performing power control at FD BSs and show that reducing their power avoids UL degradation, while still enabling to enhance the DL performance with respect to a HD deployment.

The paper is organized as follows. In Section II the model is introduced. Section III shows the system's analytical performance. Section IV shows numerical results and system design insights are provided. Finally, Section V concludes the paper.

II. System Model

A. Stochastic Geometry-Based Model

We consider a cellular network in which BSs are placed following an homogeneous PPP, Φ, of spatial density λ and the location of users follows an independent homogeneous PPP, $\tilde{\Phi}$, of density $\tilde{\lambda}$. UEs are connected to their closest BS and we take into account the following assumption.

Assumption 1. *We assume that $\tilde{\lambda} \gg \lambda$. Hence, the probability of having at least two users inside the coverage area of each BS is close to 1.*

Given possible implementation difficulties, we assume that UEs are strictly HD elements, thus they can only transmit or receive data in a given resource-block (RB). This idea is supported by the findings in [9], which state that a network can still benefit from FD gains even without FD users. Yet, BSs are capable of operating both in HD- and FD-mode, with p being the probability that a BS adopts FD-mode. Consequently, there is an homogeneous PPP, Φ_H, of density $(1-p)\lambda$ describing the position of HD BSs and another, Φ_F, of density $p\lambda$ for FD BSs. Furthermore, we define Ψ_H and Ψ_F as the set of UL users linked to HD- and FD-enabled BSs, respectively. Note that Ψ_H and Ψ_F are not necessarily homogeneous PPPs and that they depend on processes Φ_H and Φ_F, respectively, as the position of an active UE relies on the scheduling decision and location of the BS to which it is linked.

To improve readability, in the sequel, BSs are designated with x's and UEs with y's. Additionally, u and d represent UL and DL, thus y_u and y_d refer to users in UL and DL, respectively. Moreover, F and H represent FD- and HD-mode.

B. Scheduling Model

Let $\daleth$ be the set of all RBs over the system bandwidth, B, during one radio frame. $\daleth$ is partitioned into two subsets, such that $\daleth_{\text{UL}} \cap \daleth_{\text{DL}} = \emptyset$ and $\daleth_{\text{UL}} \cup \daleth_{\text{DL}} = \daleth$. Given Assumption 1, every BS has at least one UL and one DL user to serve using two generic RB, $\tau_u \in \daleth_{\text{UL}}$ and $\tau_d \in \daleth_{\text{DL}}$. If a BS adopts the HD-mode, in every instant it serves two of its users in an orthogonal manner, where the UL takes place in τ_u and the DL in τ_d, without interfering between each other. On the other hand, when FD is adopted, τ_u and τ_d can be used simultaneously for UL and DL, hence the BS informs its users that they can operate in both RBs, immediately doubling the available transmission bandwidth if compared to HD-mode.

Given the previously introduced setting, if we consider that $y_u^{(k)}$ and $y_d^{(k)}$ are served by $x^{(k)}$, and $y_d^{(0)}$ is a typical DL user connected to BS $x^{(0)}$, we can notice that in general:

$$D(y_d^{(0)}, x^{(k)}) \gg D(y_u^{(k)}, x^{(k)}), \quad \forall k \neq 0,$$

where $D(q, v)$ is the distance between two network elements q and v. Hence, we proceed to assume the following.

Assumption 2. *The distance between a typical DL user, $y_d^{(0)}$, and a random interferer, $y_u^{(k)}$, can be approximated by the distance separating $y_d^{(0)}$ and the BS serving $y_u^{(k)}$, i.e. $x^{(k)}$. Thus:*

$$D(y_d^{(0)}, y_u^{(k)}) \approx D(y_d^{(0)}, x^{(k)}). \tag{1}$$

Notice that with (1) and given the fact that in each instant there is one active UL user per cell, Ψ_H and Ψ_F become two independent homogeneous PPPs of densities $(1-p)\lambda$ and $p\lambda$, respectively.

C. Transmission Characteristics

We assume that all users transmit at their maximum power capabilities, P_u, while, a BS's transmission power is given by:

$$P = \begin{cases} \rho P_d, & \forall x^{(k)} \in \Phi_F, \\ P_d, & \text{otherwise}, \end{cases}$$

where $\rho \in (0, 1]$ serves as power control parameter to FD-enabled BSs.

Given the nature of mmWave transmissions we use directional beamforming to cope with the larger path-loss degradation dependency. In this case, beamforming aims as well to reduce the intra- and inter-cell interference observed in FD-based networks. We implement directional antennas both in BSs and UEs and the antenna gain is given by [5]–[8]:

$$G_e(\theta) = \begin{cases} G_e^{(\max)}, & \text{if } |\theta| \leq \omega_e, \\ G_e^{(\min)}, & \text{otherwise}, \end{cases} \tag{2}$$

where $e \in \{\text{BS,UE}\}$, $\theta \in [-\pi, \pi)$ is the angle of the boresight direction, ω_e is the beamwidth of the main lobe, $G_e^{(\max)}$ and $G_e^{(\min)}$ are the array gains of the main and side lobes, respectively. Further, we assume that all elements are able to perfectly estimate their steering angles towards their linked counterpart. Hence, for an intended link the antenna gain is given by $G^{(\max)} = G_{\text{BS}}^{(\max)} G_{\text{UE}}^{(\max)}$.

It is important to note that when analyzing the DL performance in traditional HD-based systems we only consider

BS-to-UE interference, and on the other hand, for the UL, UE-to-BS interference is taken into account. Yet in our case, due to the existence of FD connections, for the DL there are BS-to-UE and UE-to-UE interferences, and for the UL, UE-to-BS and BS-to-BS. Let $G(q, v)$ be the antenna gain product between a network element v and any interferer q. We assume that the beams of interfering links are uniformly distributed with respect to each other in $[-\pi, \pi)$. Hence, the gain $G(q, v)$ is randomly distributed [7].

Furthermore, given the fact that FD-enabled BSs simultaneously receive and transmit signals, they can be described by two lobes; one pointing towards the DL user and the other in the direction of the UL. Hence, from (2) we can measure the angle between these two lobes for any BS $x^{(k)}$ as:

$$\Delta\theta^{(k)} = \left|\theta_u^{(k)} - \theta_d^{(k)}\right|,$$

where $\theta_u^{(k)}$ and $\theta_d^{(k)}$ are the UL and DL angles of the boresight directions, respectively. By considering $\Delta\theta^{(k)}$ and (2), we are able to write the RSI of a FD-enabled BS as:

$$\text{RSI} = \begin{cases} \underbrace{\beta G_{\text{BS}}^{(\min)} G_{\text{BS}}^{(\max)}}_{\alpha} \rho P_d, & \text{if } \Delta\theta^{(k)} > \omega_{\text{BS}}, \\ \underbrace{\beta (G_{\text{BS}}^{(\max)})^2}_{\tilde{\beta}} \rho P_d, & \text{otherwise,} \end{cases} \tag{3}$$

where $\beta \geq 0$ is a constant related to the self-IC technique used at the BS transceiver. From (3), we can firstly notice that the term $\beta\rho P_d$ corresponds to the same RSI model used in [1]. Secondly, that $\tilde{\beta} \geq \alpha \geq 0$, thus the RSI is further reduced at those BSs that have non-interfering beams. And, lastly, that $\tilde{\beta} \geq \alpha \geq \beta$, hence due to the antenna gains, mmWave FD-enabled BSs may experience higher RSI values when compared to a sub-6 GHz case.

D. Propagation and Channel Model

Given the nature of mmWaves propagation, we consider that links can be in LOS, NLOS or outage (OUT) state. LOS happens when there is a direct and unobstructed path between transmitter and receiver. NLOS occurs when the previous path is obstructed, and finally, an outage state refers to the case in which the link can not actually be set. For the first two states, we define a path-loss function [7], [14]:

$$\ell_s(r) = (\kappa_s\, r)^{\eta_s},$$

where $s \in \{\text{LOS,NLOS}\}$, κ_s is the links' reference path-loss at 1 meter, η_s is the path-loss exponent and r the link distance. Particularly, for an OUT link state, the path-loss is equal to ∞. In the sequel, we use a plain 'ℓ' to refer to any possible link state and $\ell(v, q)$ to define the path-loss between v and q.

The probability of occurrence of each link state is given by [7], [15]:

$$\begin{aligned} p_{\text{OUT}}(r) &= \max\{0, 1 - \xi_{\text{OUT}} \exp(-\zeta_{\text{OUT}} r)\} \\ p_{\text{LOS}}(r) &= (1 - p_{\text{OUT}}(r))\xi_{\text{LOS}} \exp(-\zeta_{\text{LOS}} r) \\ p_{\text{NLOS}}(r) &= (1 - p_{\text{OUT}}(r))(1 - \xi_{\text{LOS}} \exp(-\zeta_{\text{LOS}} r)), \end{aligned}$$

where $(\xi_{\text{OUT}}, \zeta_{\text{OUT}})$ and $(\xi_{\text{LOS}}, \zeta_{\text{LOS}})$ are variables that depend on the environment and on the system's operation frequency.

Additionally, shadowing is considered and the channel power variations follow a Log-Normal distribution with means μ_s and standard deviations σ_s, where $s \in \{\text{LOS, NLOS}\}$. We refer to $|h_s|^2$ as the channel gain of an intended link and we use $|h(q, v)|^2$ to define the channel gain between network elements q and v. Let us recall that by considering shadowing, the BS serving a given UE may not necessarily be the best server at a given instant, as users are linked to their closest BS. Yet shadowing is accounted to model more precisely the channel characteristic in mmWave environments. Moreover, results in [7, Fig. 8] show that the performance of cell association based on the highest received power and closest BS are similar, validating our choice.

Given the network's topology, we can consider that the set of all path-losses form a PPP, $L = \{L_{\text{LOS}}, L_{\text{NLOS}}, L_{\text{OUT}}\}$, with intensity measure, $\Lambda_L([0, x))$, defined as [7, Lemma 1]:

$$\Lambda_L([0, x)) = \Lambda_{L_{\text{LOS}}}([0, x)) + \Lambda_{L_{\text{NLOS}}}([0, x)),$$

where $\Lambda_{L_{\text{LOS}}}([0, x)) = \Upsilon_0(x; \text{LOS})$ and $\Lambda_{L_{\text{NLOS}}}([0, x)) = \Upsilon_1(x; \text{NLOS}) - \Upsilon_0(x; \text{NLOS})$, with $\Upsilon_0(x; s)$ and $\Upsilon_1(x; s)$ defined at the top of next page, $\mathcal{H}(\cdot)$ being the Heaviside function, $\bar{\mathcal{H}}(x) = 1 - \mathcal{H}(x)$, $\mathcal{K}_1 = 2\pi\lambda\xi_{\text{LOS}}\zeta_{\text{LOS}}^{-2}$, $\mathcal{K}_2 = 2\pi\lambda\xi_{\text{LOS}}\xi_{\text{OUT}}(\zeta_{\text{LOS}} + \zeta_{\text{OUT}})^{-2}$, $R = \zeta_{\text{LOS}}\zeta_{\text{OUT}}^{-1} \ln(\xi_{\text{OUT}})$, $W = (\zeta_{\text{LOS}} + \zeta_{\text{OUT}})\zeta_{\text{OUT}}^{-1} \ln(\xi_{\text{OUT}})$, $Q_s = \zeta_{\text{LOS}}\kappa_s^{-1}$, $T_s = \zeta_{\text{OUT}}\kappa_s^{-1}$, $V_s = (\zeta_{\text{LOS}} + \zeta_{\text{OUT}})\kappa_s^{-1}$ and $Z_s = (\kappa_s\zeta_{\text{OUT}}^{-1} \ln(\xi_{\text{OUT}}))^{\eta_s}$. Furthermore, the path-loss of an intended link can be expressed as: $L^{(0)} = \min\{L_{\text{LOS}}^{(0)}, L_{\text{NLOS}}^{(0)}, L_{\text{OUT}}^{(0)}\}$, as UEs are connected to their closest BS.

E. Signal-to-Interference-plus-Noise Ratio (SINR) Formulation

1) UL SINR: We can write the UL SINR at RB τ_u, when a typical BS $x^{(0)}$ is connected to UE $y_u^{(0)}$ as:

$$\gamma_{\tau_u, u} = \frac{G^{(\max)} P_u |h_s|^2 L^{(0)}(r)^{-1}}{I_{H,u}^{(u)} + I_{F,u} + I_{\text{RSI}}\, \mathbb{1}_{[x^{(0)} \in \Phi_F]} + \sigma^2}, \tag{4}$$

where $s \in \{\text{LOS, NLOS}\}$, r is the link distance,

$$I_{H,u}^{(u)} = \sum_{j \in \mathcal{Y}_H} G(j, x^{(0)})\; P_u\; |h(j, x^{(0)})|^2\; \ell(j, x^{(0)})^{-1}$$

is the interference coming from HD ULs (where $\mathcal{Y}_H = \Psi_H$ if $x^{(0)} \in \Phi_F$, otherwise $\mathcal{Y}_H = \Psi_H \backslash y_u^{(0)}$),

$$\begin{aligned} I_{F,u} = &\sum_{i \in \mathcal{X}_F} G(i, x^{(0)})\; \rho P_d\; |h(i, x^{(0)})|^2\; \ell(i, x^{(0)})^{-1} \\ &+ \sum_{j \in \mathcal{Y}_F} G(j, x^{(0)})\; P_u\; |h(j, x^{(0)})|^2\; \ell(j, x^{(0)})^{-1} \end{aligned}$$

is the interference coming from FD links (where $\mathcal{X}_F = \Phi_F$ if $x^{(0)} \in \Phi_H$, otherwise $\mathcal{X}_F = \Phi_F \backslash x^{(0)}$, and $\mathcal{Y}_F = \Psi_F$ if $y_u^{(0)} \in \Psi_H$, otherwise $\mathcal{Y}_F = \Psi_F \backslash y_u^{(0)}$), I_{RSI} is the RSI expression given in (3) and σ^2 is the noise power. Furthermore, the UL SINR at RB τ_d is given by:

$$\gamma_{\tau_d, u} = \frac{G^{(\max)} P_u |h_s|^2 L^{(0)}(r)^{-1}}{I_{H,d}^{(u)} + I_{F,u} + I_{\text{RSI}} + \sigma^2}, \tag{5}$$

$$\Upsilon_0(x;s) = \mathcal{K}_2\left(e^{-W} + We^{-W} - e^{-V_s x^{1/\eta_s}} - V_s x^{1/\eta_s} e^{-V_s x^{1/\eta_s}}\right)\mathcal{H}(x-Z_s)$$
$$+\mathcal{K}_1\left(1 - e^{-Q_s x^{1/\eta_s}} - Q_s x^{1/\eta_s} e^{-Q_s x^{1/\eta_s}}\right)\bar{\mathcal{H}}(x-Z_s) + \mathcal{K}_1\left(1 - e^{-R} - Re^{-R}\right)\mathcal{H}(x-Z_s)$$
$$\Upsilon_1(x;s) = \pi\lambda\kappa_s^{-2} x^{2/\eta_s}\bar{\mathcal{H}}(x-Z_s) + \pi\lambda\left(\zeta_{\text{OUT}}^{-1}\ln\left(\xi_{\text{OUT}}\right)\right)^2\mathcal{H}(x-Z_s)$$
$$+2\pi\lambda\zeta_{\text{OUT}}^{-2}\xi_{\text{OUT}}\left(\xi_{\text{OUT}}^{-1} + \xi_{\text{OUT}}^{-1}\ln\left(\xi_{\text{OUT}}\right) - e^{-T_s x^{1/\eta_s}} - T_s x^{1/\eta_s} e^{-T_s x^{1/\eta_s}}\right)\mathcal{H}(x-Z_s)$$

where

$$I_{H,d}^{(u)} = \sum_{i\in\Phi_H} G(i,x^{(0)})\ P_d\ |h(i,x^{(0)})|^2\ \ell(i,x^{(0)})^{-1}$$

is the interference coming from HD DLs. Let us recall that we only have UL transmissions at τ_d when $x^{(0)} \in \Phi_F$.

2) DL SINR: The DL SINR at RB τ_d can be written as:

$$\gamma_{\tau_d,d} = \frac{G^{(\max)} P |h_s|^2 L^{(0)}(r)^{-1}}{I_{H,d}^{(d)} + I_{F,d} + \sigma^2}, \tag{6}$$

where $s \in \{\text{LOS, NLOS}\}$, $I_{H,d}^{(d)}$ is the interference coming from HD DLs and is equal to $I_{H,d}^{(u)}$ yet the interference is calculated towards $y_d^{(0)}$ instead of $x^{(0)}$, and

$$I_{F,d} = \sum_{i\in\mathcal{X}_F} G(i,y_d^{(0)})\ \rho P_d\ |h(i,y_d^{(0)})|^2\ \ell(i,y_d^{(0)})^{-1}$$
$$+\sum_{j\in\Psi_F} G(j,y_d^{(0)})\ P_u\ |h(j,y_d^{(0)})|^2 \ell(j,y_d^{(0)})^{-1}$$

is the interference coming from FD links. Furthermore, the DL SINR at RB τ_u can be written as:

$$\gamma_{\tau_u,d} = \frac{G^{(\max)} P |h_s|^2 L^{(0)}(r)^{-1}}{I_{H,u}^{(d)} + I_{F,d} + \sigma^2}, \tag{7}$$

where $I_{H,u}^{(d)}$ is the interference coming from HD ULs and is equal to $I_{H,u}^{(u)}$ yet the interference is calculated towards $y_d^{(0)}$ instead of $x^{(0)}$. Let us recall once again, that a DL transmission occurs at τ_u if and only if $x^{(0)} \in \Phi_F$.

F. Coverage Probability Formulation

The coverage probability, $\mathcal{P}$, is defined as:

$$\mathcal{P}(T,\tau_m,\tilde{m}) = \mathbb{P}\left(\gamma_{\tau_m,\tilde{m}} > T\right) \tag{8}$$

for $(m,\tilde{m}) \in \{u,d\}$. Additionally, for each duplex-mode, the coverage probability can be expressed as:

$$\mathcal{P}^{(\text{mode})}(T,\tau_m,\tilde{m}) = \mathcal{P}_{\text{LOS}}^{(\text{mode})}(T,\tau_m,\tilde{m}) + \mathcal{P}_{\text{NLOS}}^{(\text{mode})}(T,\tau_m,\tilde{m}),$$

where mode $\in \{F,H\}$ and, $\mathcal{P}_{\text{LOS}}$ and $\mathcal{P}_{\text{NLOS}}$ depend on the probability of occurrence of each link state and are further defined in Proposition 1 and Theorem 1. Hence, by recalling that we only have an UL at τ_d and a DL at τ_u, when $x^{(0)} \in \Phi_F$, we can write $\mathcal{P}$ in (8) as:

$$\begin{cases} p\ \mathcal{P}^{(F)}(T,\tau_m,\tilde{m}) + (1-p)\ \mathcal{P}^{(H)}(T,\tau_m,\tilde{m}), & \text{if } m=\tilde{m}, \\ \mathcal{P}^{(F)}(T,\tau_m,\tilde{m}), & \text{otherwise.} \end{cases}$$

G. Spectral Efficiency Formulation

We define the instantaneous SE, $\mathcal{S}$, for UL and DL, in a cell defined by a typical BS $x^{(0)}$ as:

$$\mathcal{S}_m = \begin{cases} \sum\limits_{\tilde{m}\in\{u,d\}} \log_2\left(1+\gamma_{\tau_{\tilde{m}},m}\right), & \text{if } x^{(0)} \in \Phi_F, \\ \log_2\left(1+\gamma_{\tau_m,m}\right), & \text{otherwise.} \end{cases}$$

where $m \in \{u,d\}$. Further, the ASE, hereafter written as $\mathcal{A}$, can be defined as the expected value of $\mathcal{S}_m$, where the average is taken over the different SINR distributions. Then:

$$\mathcal{A}_m(p,\rho) = \frac{1}{2}\Big(p\sum_{\tilde{m}\in\{u,d\}} \mathbb{E}_{\gamma_{\tau_{\tilde{m}},m}}\left[\log_2\left(1+\gamma_{\tau_{\tilde{m}},m}\right) \mid x^{(0)} \in \Phi_F\right]$$
$$+ (1-p)\mathbb{E}_{\gamma_{\tau_m},m}\left[\log_2\left(1+\gamma_{\tau_m,m}\right) \mid x^{(0)} \in \Phi_H\right]\Big), \tag{9}$$

where term $1/2$ appears due to the fact that one RB uses half of the total available transmission bandwidth in a given instant. Let us notice that the first addend in (9) represents the ASE of the FD part, whereas the second, the HD contribution. The ASE of a typical cell, $\mathcal{A}_c$, is defined as: $\mathcal{A}_u + \mathcal{A}_d$.

Finally, we express the ASE gain with respect to a traditional HD network, i.e. $(p,\rho) = (0,\cdot)$, by:

$$\mathcal{F}_m(p,\rho) = \frac{\mathcal{A}_m(p,\rho)}{\mathcal{A}_m(0,\cdot)}.$$

III. Analytical Performance Analysis

In order to allow tractability of the analytical expressions, we consider for the sequel the following assumption.

Assumption 3. *The interference from a network element (BS or UE) to another is negligible.*

Let us recall that this assumption does not suppress the RSI in the FD's UL, nor the presence of noise. The accuracy of all assumptions is validated in Section IV.

A. Coverage Probability

With Assumption 3, the DL SINRs in (6) and (7) are:

$$\gamma_{\tau_m,d} = \frac{G^{(\max)} P |h_s|^2}{\sigma^2 L^{(0)}},$$

where $m \in \{u,d\}$ and $s \in \{\text{LOS,NLOS}\}$. For the UL, the SINRs in (4) and (5) are:

$$\gamma_{\tau_m,u} = \frac{G^{(\max)} P_u |h_s|^2}{(I_{\text{RSI}}\ \mathbb{1}_{[x^{(0)}\in\Phi_F]} + \sigma^2) L^{(0)}}.$$

$$\dot{\Upsilon}_0(x;s) = \mathcal{K}_2(V_s^2/\eta_s)x^{2/\eta_s-1}e^{-V_s x^{1/\eta_s}}\mathcal{H}(x-Z_s) + \mathcal{K}_1(Q_s^2/\eta_s)x^{2/\eta_s-1}e^{-Q_s x^{1/\eta_s}}\bar{\mathcal{H}}(x-Z_s)$$
$$\dot{\Upsilon}_1(x;s) = 2\pi\lambda\kappa_s^{-2}\eta_s^{-1}x^{2/\eta_s-1}\bar{\mathcal{H}}(x-Z_s) + 2\pi\lambda\zeta_{\text{OUT}}^{-2}\xi_{\text{OUT}}T_s^2\eta_s^{-1}x^{2/\eta_s-1}e^{-T_s x^{1/\eta_s}}\mathcal{H}(x-Z_s)$$

Proposition 1 (Coverage probability for DL in HD- and FD-mode, and UL in HD-mode)**.**

$$\mathcal{P}_s^{(\text{mode})}(T,\tau_m,\tilde{m}) = \int_0^\infty Q\Big(\ln\big(Tx\frac{\sigma^2}{G^{(\max)}\tilde{P}}\big) - \mu_s\Big) \cdot\dot{\Lambda}_{L_s}([0,x))\exp\left(-\Lambda_L([0,x))\right)dx, \quad (10)$$

where $s \in \{\text{LOS,NLOS}\}$*,* $Q(\cdot)$ *is the Q-function,* $(\text{mode},m,\tilde{m}) \in \{(H,d,d),\ (H,u,u),\ (F,d,d),\ (F,u,d)\}$*,*

$$\tilde{P} = \begin{cases} P, & \text{if } \tilde{m} = d, \\ P_u, & \text{otherwise,} \end{cases}$$

$\dot{\Lambda}_{L_s}(\cdot)$ *is the derivative of* Λ_{L_s} *with respect to* x*,*

$$\dot{\Lambda}_{L_{\text{LOS}}}([0,x)) = \dot{\Upsilon}_0(x;\text{LOS}),$$
$$\dot{\Lambda}_{L_{\text{NLOS}}}([0,x)) = \dot{\Upsilon}_1(x;\text{NLOS}) - \dot{\Upsilon}_0(x;\text{NLOS}),$$

with $\dot{\Upsilon}_0(\cdot;\cdot)$ *and* $\dot{\Upsilon}_1(\cdot;\cdot)$ *expressed at the top of this page.*

Proof: Straightforward application of [7, Proposition 1] to our model. ∎

Theorem 1 (Coverage probability for UL in FD-mode)**.**

$$\mathcal{P}_s^{(F)}(T,\tau_m,u) = \int_0^\infty \Bigg[Q\Big(\ln\big(Tx\frac{\alpha P+\sigma^2}{G^{(\max)}P_u}\big) - \mu_s\Big)\frac{(2\pi-\omega_{BS})^2}{(2\pi)^2} + Q\Big(\ln\big(Tx\frac{\tilde{\beta}P+\sigma^2}{G^{(\max)}P_u}\big) - \mu_s\Big)\Big(1 - \frac{(2\pi-\omega_{BS})^2}{(2\pi)^2}\Big)\Bigg] \cdot \dot{\Lambda}_{L_s}([0,x))\exp\left(-\Lambda_L([0,x))\right)dx, \quad (11)$$

where $s \in \{\text{LOS,NLOS}\}$ *and* $m \in \{u,d\}$*.*

Proof: See Appendix A. ∎

B. Average Spectral Efficiency

Theorem 2 (ASE)**.** *Given (9), (10) and (11), the ASE of a link is:*

$$\mathcal{A}_m = \frac{1}{2}\Big[p\sum_{\tilde{m}\in\{u,d\}}\int_0^\infty \frac{\mathcal{P}^{(F)}(T,\tau_{\tilde{m}},m)}{\ln(2)(1+T)}\,dT + (1-p)\int_0^\infty \frac{\mathcal{P}^{(H)}(T,\tau_m,m)}{\ln(2)(1+T)}\,dT\Big], \quad (12)$$

where $m \in \{u,d\}$*.*

Proof: From positivity of $\gamma_{\tau_{\tilde{m}},m}$, $\forall(m,\tilde{m}) \in \{u,d\}$, $\mathbb{E}_{\gamma_{\tau_{\tilde{m}},m}}\left[\log_2(1+\gamma_{\tau_{\tilde{m}},m})\right]$ can be written as:

$$\int_0^\infty \mathbb{P}\left(\log_2(1+\gamma_{\tau_{\tilde{m}},m}) > T\right)dT = \int_0^\infty \frac{\mathbb{P}\left(\gamma_{\tau_{\tilde{m}},m} > T\right)}{\ln(2)(1+T)}\,dT.$$

∎

TABLE I
SIMULATION PARAMETERS

Parameter	Value	Parameter	Value
B	400 MHz	RB bandwidth	720 KHz
P_d	30 dBm	P_u	23 dBm
β	-100 dB	$\omega_{\text{BS}} = \omega_{\text{UE}}$	30°
$G_{\text{BS}}^{(\max)} = G_{\text{UE}}^{(\max)}$	20 dB	$G_{\text{BS}}^{(\min)} = G_{\text{UE}}^{(\min)}$	-10 dB
$(\kappa_{\text{LOS}}, \eta_{\text{LOS}})$	(30.7 dB, 2)	$(\kappa_{\text{NLOS}}, \eta_{\text{NLOS}})$	(24.66 dB, 2.92)
$(\xi_{\text{LOS}}, \zeta_{\text{LOS}})$	(1, 1/67.1)	$(\xi_{\text{OUT}}, \zeta_{\text{OUT}})$	(exp (5.2), 1/30)
$(\mu_{\text{LOS}}, \sigma_{\text{LOS}})$	(0, 5.8 dB)	$(\mu_{\text{NLOS}}, \sigma_{\text{NLOS}})$	(0, 8.7 dB)
Noise figure	10 dB	Noise density	-174 dBm/Hz
$(\sigma_{\text{LOS}}, \sigma_{\text{NLOS}})$	(5.8, 8.7)dB	R_c	100 m

IV. SIMULATION AND PERFORMANCE EVALUATION

We focus our analysis in the 28 GHz band, given the interest of commercial deployments for 5G in this part of the spectrum. We simulate the network according to Table I which is based on [15], [16]. Contrary to the analytical framework, simulations take into account all interferences. Knowing that in a PPP-based network the average distance between a BS and its closest counterpart is $(2\sqrt{\lambda})^{-1}$, we define the average cell radius as: $R_c = (4\sqrt{\lambda})^{-1}$. For comparison, we simulate a sub-6 GHz network according to the urban micro-cell model in [17], with central carrier frequency of 2.6 GHz, path-loss functions $\ell_{\text{LOS}}(r) = 28 + 22\log_{10}(r) + 20\log_{10}(2.6)$ and $\ell_{\text{NLOS}}(r) = 22.7 + 36.7\log_{10}(r) + 26\log_{10}(2.6)$, shadowing standard deviations $\sigma_{\text{LOS}} = 3$ dB and $\sigma_{\text{NLOS}} = 4$ dB, $p_{\text{LOS}}(r) = \min(18/r, 1)(1 - \exp(-r/36)) + \exp(-r/36)$, $p_{\text{OUT}} = 0$, $B = 20$ MHz and omnidirectional antennas.

Fig. 1 shows the coverage probability, $\mathcal{P}(T,\tau_m,\tilde{m})$, as a function of T, for different values of p. We observe that simulated and analytical results match well, supporting all previous Assumptions. Results also show that DL outperforms UL, which under the validation of Assumption 3, is explained by the fact that $P_d > P_u$. Further, by focusing in the UL (Fig. 1 (a)), we see that τ_u outperforms τ_d. This was expected as τ_d is only used by BSs in FD-mode, hence the RSI is always considered, whereas τ_u is also used by HD BSs (with no RSI), consequently enhancing the performance. Regarding the DL in Fig. 1 (b), we see that the all-HD and all-FD (with $\rho = 1$) curves, almost match. Validating again Assumption 3. Yet the curves do not match exactly, as there is a remaining interference generated by the overture of antennas, ω_e.

Fig. 2 shows the coverage probability as a function of ρ, for different values of p. For the UL in Fig. 2 (a), we see that for a fixed ρ and $T = -10$ dB, the performance of τ_u decreases with p, yet not due to interference coming from other links (as Assumption 3 was validated), but to the adoption of FD which generates RSI. This is clearly proven by the perfect self-IC case ($\beta = 0$), where the UL coverage probability is constant

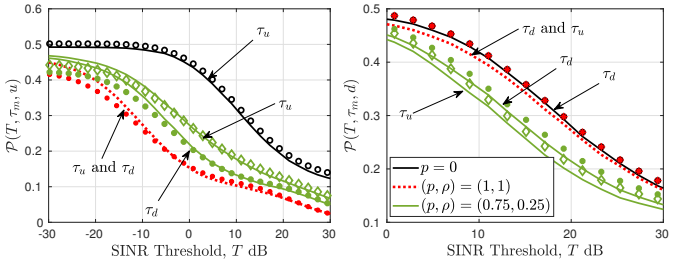

(a) UL coverage probability. (b) DL coverage probability.

Fig. 1. Coverage probability, $\mathcal{P}(T,\tau_m,\tilde{m})$. Markers are for analytical results.

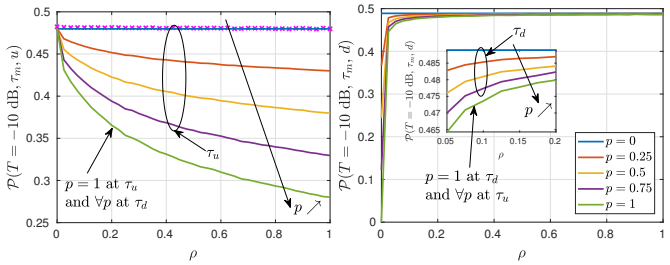

(a) UL coverage probability vs. ρ. (b) DL coverage probability vs. ρ.

Fig. 2. Coverage probability for $T=-10$ dB. Markers are for $\beta=0$.

for all p's. The previous argument is further supported by the behavior of τ_d (only used by FD BSs) which does not vary with p. Concerning the impact of ρ, a similar conclusion is derived, as greater ρ's generate a higher RSI, degrading the UL performance. Thus, in terms of UL coverage probability, smaller values of p and ρ are preferable.

For the DL in Fig. 2 (b), the performance of both τ_u and τ_d is practically independent of p, since the inter-cell interference is negligible compared a sub-6 GHz case [1]. The slight dependence on p for τ_d happens at extremely small values of ρ, where the transmission power of FD DLs is heavily reduced. Further, the performance is enhanced with ρ, as transmit and receive power increase with ρ on the DL without adding interference, as in sub-6 GHz. Thus, for the DL coverage probability higher values of p and ρ are preferable.

The ASE performance of the system for different (p,ρ,β) configurations is depicted in Fig. 3. As it is for the coverage probability, Fig. 3 (a) shows that for the UL small values of ρ and p are preferable, whereas for the DL and cell, in Fig. 3 (c) and (d), it is the opposite. For $\beta=0$ in Fig. 3 (b), the UL performance is independent of ρ (also seen in Fig. 2 (a)), since there is no RSI, but it grows with p, as FD always outperforms HD in terms of ASE if the noise-plus-interference is the same for both cases. Additionally, results confirm that an hybrid FD/HD deployment is not required in mmWave, since the links are maximized for $p=1$ or $p=0$. Yet it demonstrates the interest of performing power control at FD BSs with imperfect self-IC ($\beta\neq 0$). We can indeed observe that for $\rho=0.1$, the UL ASE remains almost unchanged, while still enabling an enhancement of the DL performance.

Table II (a) shows the ASE performance of HD networks in sub-6 GHz and 28 GHz, noticing a superiority of mmWaves. Table II (b) presents the links' ASEs for a sub-6 GHz network where all BSs are in FD-mode, for different β's and no power control. Results show that if $\beta\neq 0$ the UL is heavily degraded ($\mathcal{F}_u=0.67$). Table II (c) also displays the links' ASEs for an all-FD network, yet by considering our model for different ρ's and β's. As with HD, mmWave also increases the ASE of FD networks. In fact, for $\beta=-100$ dB, if $\rho=0.13$, there is an enhancement of 133% in the UL, 85% in the DL and 100% in the cell. Moreover, UL degradation is avoided ($\mathcal{F}_u=1$), while still enhancing the DL and cell performances ($\mathcal{F}_d=1.36$ and $\mathcal{F}_c=1.21$). Additionally, for $\beta=0$, each link almost doubles the performance of the HD system, closely approaching the ASE of an ideal FD system ($\mathcal{F}_m=2$).

As FD enhances the system's ASE, an operator may be interested in relaxing its coverage probability floor level. In this regard, it is possible to find a $\rho=\rho^*$, such that $\rho_{\text{DL}}^{(\min)}\leq\rho^*\leq\rho_{\text{UL}}^{(\max)}$, where $\rho_{\text{DL}}^{(\min)}$ is the minimum acceptable ρ to achieve the expected DL coverage probability and $\rho_{\text{UL}}^{(\max)}$ is the biggest ρ to obtain a given UL coverage probability threshold. As an example, let us suppose that an operators tolerates a coverage probability loss at $T=-10$ dB of 20% and 10% in the UL and DL, respectively, when compared to a HD network. By analyzing Fig. 2, $\rho_{\text{UL}}^{(\max)}=0.15$ and $\rho_{\text{DL}}^{(\min)}=0.025$. If the operator's interest is to favor the UL performance, $\rho^*=\rho_{\text{DL}}^{(\min)}$, while for a DL maximization $\rho^*=\rho_{\text{UL}}^{(\max)}$. Table II (d), shows the ASEs for this cases, observing that in each configuration it is not possible to improve the performance of all links simultaneously. In this regard for a $\rho^*=(\rho_{\text{DL}}^{(\min)}+\rho_{\text{UL}}^{(\max)})/2$, we see in Table II (e) that all links outperform their HD counterpart.

V. Conclusions

In this paper we study a beamforming-based mmWave cellular network, where BSs are capable of switching between half- and full-duplex. The analysis is carried out by using stochastic geometry and a realistic channel model. Primary results show that mmWave-based networks outperform sub-6 GHz ones in terms of spectral efficiency. We also prove that hybrid FD/HD deployments are not required in mmWave and that if FD BSs are not capable of perfectly canceling their self-interference, reducing their transmission power avoids UL degradation, while still enabling a DL spectral efficiency improvement with respect to a mmWave HD system.

Appendix A

Proof of Theorem 1

By using Proposition 1 and considering that I_{RSI} is a random variable we can write $\mathcal{P}_s^{(F)}(T,\tau_m,u)$ as:

$$\mathbb{E}_{I_{\text{RSI}}}\left[\int_0^\infty \underbrace{Q\Big(\ln\big(Tx\frac{(I_{\text{RSI}}+\sigma^2)}{G^{(\max)}P_u}\big)-\mu_s\Big)}_{\mathbb{Q}_s(I_{\text{RSI}})}\right.$$

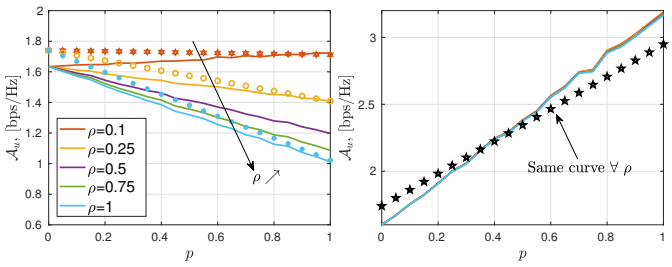

(a) UL ASE vs. p, for $\beta = -100$ dB. (b) UL ASE vs. p, for $\beta = 0$.

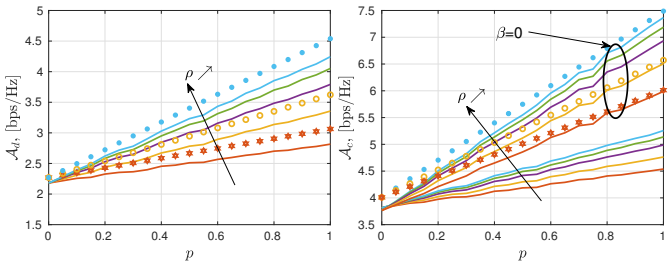

(c) DL ASE vs. p. (d) Cell ASE vs. p.

Fig. 3. ASE performances. Markers are for analytical results.

$$\cdot \underbrace{\dot{\Lambda}_{L_s}([0,x)) \exp\left(-\Lambda_L([0,x))\right)}_{\mathbb{L}_s(x)} dx \Bigg],$$

$$= \int_0^\infty \mathbb{L}_s(x)\mathbb{Q}_s(I_{\text{RSI}})\Big|_{I_{\text{RSI}}=\alpha P} \mathbb{P}\left(\Delta\theta^{(k)} > \omega_{\text{BS}}\right) dx + \int_0^\infty \mathbb{L}_s(x)\mathbb{Q}_s(I_{\text{RSI}})\Big|_{I_{\text{RSI}}=\tilde{\beta} P} \mathbb{P}\left(\Delta\theta^{(k)} \leq \omega_{\text{BS}}\right) dx$$

where $s \in \{\text{LOS},\text{NLOS}\}$, $m \in \{u, d\}$. Further, we compute $\mathbb{P}\left(\Delta\theta^{(k)} > \omega_{\text{BS}}\right)$ by considering a plane described by a square of side 2π and then calculating the surface in which the difference between two points (x, y) is greater than ω_{BS}, resulting in $\mathbb{P}\left(\Delta\theta^{(k)} > \omega_{\text{BS}}\right) = (2\pi - \omega_{\text{BS}})^2/(2\pi)^2$. ■

TABLE II

SIMULATED ASES (BPS/HZ) AND ASE GAINS WITH RESPECT TO HD ($\mathcal{F}$).

HD ASE: 2.6 GHz		
$\mathcal{A}_u$	$\mathcal{A}_d$	$\mathcal{A}_c$
1.03	1.10	2.13

HD ASE: 28 GHz		
$\mathcal{A}_u$	$\mathcal{A}_d$	$\mathcal{A}_c$
1.61	2.20	3.81

(a) HD performance under a sub-6 GHz and 28 GHz environment.

FD ASE: 2.6 GHz	$\beta = -100$ dB			$\beta = 0$		
	$\mathcal{A}_u$	$\mathcal{A}_d$	$\mathcal{A}_c$	$\mathcal{A}_u$	$\mathcal{A}_d$	$\mathcal{A}_c$
	0.69	1.62	2.30	1.21	1.62	2.83
$\mathcal{F}_m(1,\cdot)$	0.67	1.47	1.08	1.17	1.47	1.33

(b) Sub-6 GHz FD network ($p = 1$) for different β values.

FD ASE: 28 GHz	$\beta = -100$ dB, $\rho = 0.13$			$\beta = 0$, $\rho = 1$		
	$\mathcal{A}_u$	$\mathcal{A}_d$	$\mathcal{A}_c$	$\mathcal{A}_u$	$\mathcal{A}_d$	$\mathcal{A}_c$
	1.61	3.00	4.61	3.17	4.21	7.38
$\mathcal{F}_m(1,\rho)$	1.00	1.36	1.21	1.97	1.91	1.93

(c) mmWave FD network ($p = 1$) for different ρ and β values.

FD ASE: 28 GHz $\beta = -100$ dB	$\rho^* = \rho_{\text{DL}}^{(\min)} = 0.025$			$\rho^* = \rho_{\text{UL}}^{(\max)} = 0.15$		
	$\mathcal{A}_u$	$\mathcal{A}_d$	$\mathcal{A}_c$	$\mathcal{A}_u$	$\mathcal{A}_d$	$\mathcal{A}_c$
	2.22	2.11	4.33	1.55	3.06	4.61
$\mathcal{F}_m(1,\rho)$	1.38	0.96	1.14	0.96	1.39	1.21

(d) mmWave FD network ($p = 1$) for $\rho_{\text{DL}}^{(\min)}$ and $\rho_{\text{UL}}^{(\max)}$.

FD ASE: 28 GHz $\beta = -100$ dB	$\rho^* = \text{mean}(\rho_{\text{DL}}^{(\min)}, \rho_{\text{UL}}^{(\max)}) = 0.0875$		
	$\mathcal{A}_u$	$\mathcal{A}_d$	$\mathcal{A}_c$
	1.73	2.71	4.44
$\mathcal{F}_m(1,\rho)$	1.07	1.23	1.17

(e) mmWave network for $\rho = \text{mean}(\rho_{\text{DL}}^{(\min)}, \rho_{\text{UL}}^{(\max)})$.

REFERENCES

[1] H.-F. Arraño-Scharager, M. Coupechoux, and J.-M. Kelif, "Full and Half Duplex-Switching Policy for Cellular Networks under Uplink Degradation Constraint," in *IEEE International Conference on Communications*, May 2018.

[2] O. A. Ahmad AlAmmouri, Hesham ElSawy and M.-S. Alouini, "In-Band α-Duplex Scheme for Cellular Networks: A Stochastic Geometry Approach," *IEEE Transactions on Wireless Communications*, vol. 15, no. 10, pp. 6797–6812, Oct. 2016.

[3] J. Lee and T. Q. S. Quek, "Hybrid Full-/Half-Duplex System Analysis in Heterogeneous Wireless Networks," *IEEE Transactions on Wireless Communications*, vol. 14, no. 5, pp. 2883 – 2895, May 2015.

[4] W. Tang, S. Feng, Y. Liu, and Y. Ding, "Hybrid Duplex Switching in Heterogeneous Networks," *IEEE Transactions on Wireless Communications*, vol. 15, no. 11, pp. 7419 – 7431, Nov. 2016.

[5] T. Bai and R. W. Heath, "Coverage and rate analysis for millimeter wave cellular networks," *IEEE Transactions on Wireless Communications*, vol. 14, no. 2, pp. 1100 – 1114, Feb. 2015.

[6] S. Singh, M. N. Kulkarni, A. Ghosh, and J. G. Andrews, "Tractable Model for Rate in Self-Backhauled Millimeter Wave Cellular Networks," *IEEE Journal on Selected Areas in Communications*, vol. 33, no. 10, pp. 2196 – 2211, Oct. 2015.

[7] M. D. Renzo, "Stochastic Geometry Modeling and Analysis of Multi-Tier Millimeter Wave Cellular Networks," *EEE Transactions on Wireless Communications*, vol. 14, no. 9, pp. 5038 – 5057, Sep. 2015.

[8] J. G. Andrews, T. Bai, M. N. Kulkarni, A. Alkhateeb, A. K. Gupta, and R. W. Heath, "Modeling and Analyzing Millimeter Wave Cellular Systems," *IEEE Transactions on Communications*, vol. 65, no. 1, pp. 403 – 430, Jan. 2017.

[9] Z. Xiao, P. Xia, and X.-G. Xia, "Full-Duplex Millimeter-Wave Communication," *IEEE Wireless Communications*, vol. 24, no. 6, pp. 136 – 143, Dec. 2017.

[10] W. Ding, Y. Niu, H. Wu, Y. Li, and Z. Zhong, "QoS-aware Full-duplex Concurrent Scheduling for Millimeter Wave Wireless Backhaul Networks," *IEEE Access*, vol. 6, pp. 25 313 – 25 322, Apr. 2018.

[11] Z. Wei, X. Zhu, S. Sun, Y. Huang, A. Al-Tahmeesschi, and Y. Jiang, "Energy-Efficiency of Millimeter-Wave Full-Duplex Relaying Systems: Challenges and Solutions," *IEEE Access*, vol. 4, pp. 4848 – 4860, Jul. 2016.

[12] T. Dinc and H. Krishnaswamy, "Millimeter-wave full-duplex wireless: Applications, antenna interfaces and systems," in *IEEE Custom Integrated Circuits Conference (CICC)*, Apr. 2017.

[13] X. Liu, L. B. Zhenyu Xiao and, J. Choi, P. Xia, and X.-G. Xia, "Beamforming Based Full-Duplex for Millimeter-Wave Communication," *Sensors*, vol. 16, no. 7, p. 1130, Jul. 2016.

[14] B. Błaszczyszyn, M. K. Karray, and H. P. Keeler, "Using Poisson processes to model lattice cellular networks," in *Proceedings IEEE International Conference on Computer Communications (INFOCOM)*, Apr. 2013, pp. 773–781.

[15] M. R. Akdeniz, Y. Liu, M. K. Samimi, S. Sun, S. Rangan, T. S. Rappaport, and E. Erkip, "Millimeter Wave Channel Modeling and Cellular Capacity Evaluation," *IEEE Journal on Selected Areas in Communications*, vol. 32, no. 6, pp. 1164 – 1179, Jun. 2014.

[16] 3rd Generation Partnership Project (3GPP), "New frequency range for NR (24.25-29.5 GHz)," 3GPP, Tech. Rep. 3GPP TR 38.815 V0.3.0, Apr. 2018.

[17] "Evolved Universal Terrestrial Radio Access (E-UTRA); Further advancements for E-UTRA physical layer aspects (Release 9, Specification #: 36.814)," 3GPP, Tech. Rep., Mar. 2017.